Journal of Asian Earth Sciences 131 (2016) 72–80

Contents lists available at ScienceDirect

Journal of Asian Earth Sciences

journal homepage: www.elsevier.com/locate/jseaes

Full length article

Evolution of the Indian summer monsoon during the interval 32.7–11.4 cal. ka BP: Evidence from the Baoxiu peat, Yunnan, southwest China

Chao Huang [a,b], Gangjian Wei [a,*], Jinlong Ma [a], Ying Liu [a]

[a] State Key Laboratory of Isotope Geochemistry, Guangzhou Institute of Geochemistry, Chinese Academy of Sciences, Guangzhou 510640, China
[b] University of Chinese Academy of Sciences, Beijing 100039, China

ARTICLE INFO

Article history:
Received 24 June 2016
Received in revised form 11 September 2016
Accepted 14 September 2016
Available online 14 September 2016

Keywords:
Peat
East Asian summer monsoon
Indian summer monsoon
Chemical weathering

ABSTRACT

There have been few investigations of the phase relationship between the Indian summer monsoon (ISM) and the East Asian summer monsoon (EASM) during the last glacial period. We present multi-proxy mineralogical and geochemical records from a peat core taken from the Baoxiu Basin, central Yunnan, southwest China, to investigate changes in chemical weathering and climate associated with the ISM in southwest China spanning the interval ~32.7–11.4 ka BP. The results suggest that the LGM period (23–18 ka BP) was characterized by cold and dry climatic conditions. A comparison of proxy data from Baoxiu peat with other related proxy climate records reveals that broadly synchronous variations in the ISM and EASM on orbital timescales can be attributed to solar radiation forcing in the Northern Hemisphere. In addition, four synchronous weak millennial-scale monsoonal events coincide well with cooling events recorded in the NGRIP ice core (corresponding to the Younger Dryas, and Heinrich events H1, H2, and H3). Significantly, the strengths of the two Asian monsoons show an inverse relationship during the interval 23–19 ka BP, probably resulting from El Niño-like conditions in the tropical Pacific.

1. Introduction

The Indian summer monsoon (ISM) and the East Asian summer monsoon (EASM) are two subsystems of the Asian monsoon. They are independent systems but interact with each other on geological timescales (Ding and Chan, 2005). Consistencies and differences between the evolutions of these two monsoon systems indicate that they respond to both global and regional changes in climate, and knowledge of the controls on both would contribute to a better understanding of global atmospheric circulation and climate change. Indeed, recent studies have focused on the phase relationship between the evolutions of these monsoon systems during the Holocene to decipher their global and local driving forces; however, the results are debated. Zhao et al. (2009) and Zhang et al. (2011) inferred a broadly synchronous climatic evolution throughout the Holocene across the two monsoon regions by synthesizing fossil pollen and carbonate $\delta^{18}O$ records in monsoonal China. In contrast, after reviewing 75 sets of time series data from central Asia relating to Holocene moisture patterns, Herzschuh (2006) suggested the asynchronous evolution of the ISM and EASM. Meanwhile, $\delta^{13}C$ records from the Hani peat bog in northeast China and the Hongyuan peat bog in southwest China indicate an inverse phase relationship between the ISM and EASM on both orbital and millennial timescales (Hong et al., 2005, 2014b). If the timespan is extended back further to the last glacial, the phase relationship becomes even more complicated. Changes in the ISM, as inferred from pollen records from Xingyun Lake in southwest China, exhibit an out-of-phase relationship with the EASM during the last glaciation (Chen et al., 2014). Stalagmite $\delta^{18}O$ records from Sanxing Cave on the Yun-Gui Plateau show decoupling between the two monsoon systems during the interval 20–17 ka BP (Jiang et al., 2014).

Yunnan Province, located in southwest China at the southeastern edge of the Tibetan Plateau, is strongly influenced by the ISM (Shen et al., 2006; An et al., 2011; Cook et al., 2011). High-resolution paleoenvironmental records obtained from this region provide important information on the evolution and potential forcing mechanisms of the ISM. Existing studies are based mainly on lacustrine sediments with relatively low temporal resolution and covering relatively short time spans (Kramer et al., 2010; Cook et al., 2011, 2012; Tareq et al., 2011; Xiao et al., 2014a, 2014b, 2015). Indeed, only a few lacustrine records cover the period since the Last Glacial Maximum (LGM). Climatic information inferred from pollen records from Dianchi Lake and Qilu Lake suggest cold and wet conditions during the LGM (Long et al., 1991; Wu et al., 1991). Multi-proxy sediment records from Heqing Lake and

* Corresponding author.
E-mail address: gjwei@gig.ac.cn (G. Wei).

http://dx.doi.org/10.1016/j.jseaes.2016.09.008
1367-9120/

Napahai Lake also suggest a cold and wet climate during the LGM (Jiang et al., 1998; Yin et al., 2002). However, Zhu et al. (2009a) inferred cold, dry conditions from multi-proxy analysis of Lake Chen Co during the LGM. Diatom and pollen data from Lugu Lake, northwest Yunnan, indicate a dry and cold LGM (Wang et al., 2014), whereas information from a fluvial sedimentary sequence from the eastern Himalayas suggests that the climate was wet and cold during this period (Ghosh et al., 2015). These discrepancies regarding the climate of the LGM may reflect the low temporal resolution of sampling and age uncertainties.

We present an integrated set of geochemical proxy records from a peat core collected from Baoxiu Basin in central Yunnan Province, southwest China, spanning the interval 32.7–11.4 ka BP. The objectives of this study were to: (1) reconstruct the climatic evolution of the ISM during the interval 32.7–11.4 ka BP; (2) decipher the phase relationship between the ISM and EASM; and (3) clarify the timing and nature of climatic changes over the LGM in this region.

2. Geographic setting

The Baoxiu Basin (23°44′–23°47′N, 102°21′–102°23′E), a semi-enclosed basin at an altitude of ca. 1400–1430 m a.s.l., is located in central Yunnan Province, southwest China, ~150 km south of Kunming (Fig. 1). The Baoxiu Basin covers an area of ~17 km^2, with a length of 7 km and a width of 2–4 km. The regional climate is affected by the ISM and is characterized by warm, wet summers, and cold, dry winters. Based on instrumental observations from Yuxi Station, 80 km north of Baoxiu, between 1971 and 2000 (Fig. 2), mean annual precipitation in the area is 918 mm with ~76% falling between May and September.

3. Materials and methods

3.1. Core recovery and dating

A 200 cm long peat core was extracted from the margin of Chirui Lake in the Baoxiu Basin. The core was subsampled at 2 cm intervals and freeze-dried. The top 40 cm of the peat core were obviously disturbed attributed to farming. Thus, this study focuses on the sediments spanning the depth interval 41–200 cm in the core. The core chronology is based on AMS ^{14}C radiocarbon dating of five samples of grass roots (Table 1). The ages were calibrated using Calpal-2007 online software (Danzeglocke et al., 2010). The age-depth model (Fig. 3) was established by linear interpolation. For further details of the dating method and modeling approach, see Wei et al. (2012).

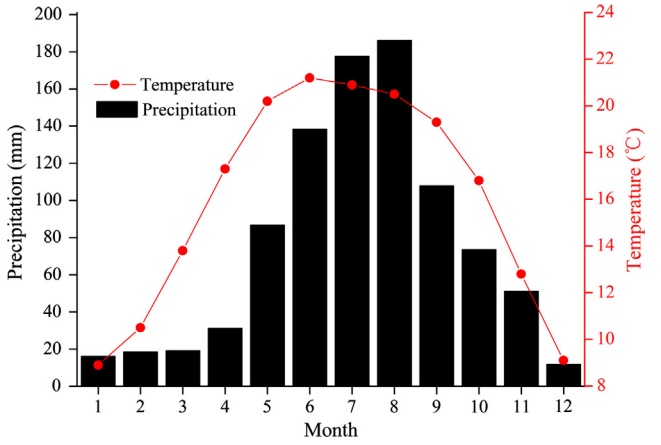

Fig. 2. Monthly mean temperature and precipitation data for the period 1971–2000, as recorded at Yuxi station.

3.2. Geochemical analysis

Samples for geochemical analysis were freeze-dried, hand-milled using a mortar, and then sieved through a 250 μm sieve. Loss on ignition (LOI) was determined by igniting the material for 2 h at 900 °C. The ash was collected for further elemental analysis, and all element concentrations were measured relative to the ash.

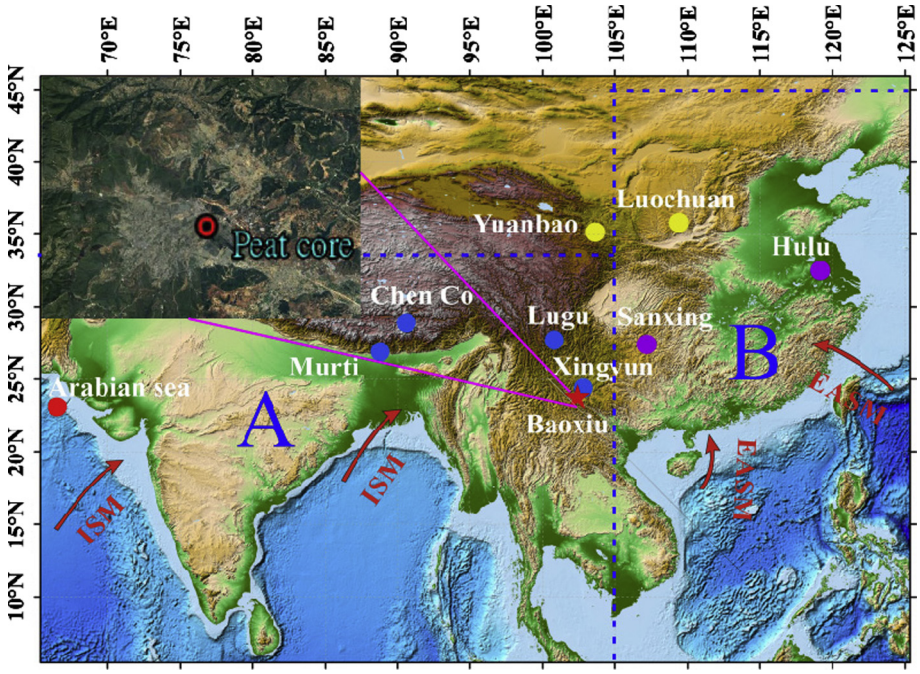

Fig. 1. Sketch map showing the location of the present research site and selected related research sites. The boxes labeled A and B define the major areas of summer precipitation; i.e., (A) the Indian summer monsoon (ISM) area, and (B) the East Asian summer monsoon (EASM) area (modified from Gao et al., 1962; Wang et al., 2003).

Table 1
AMS ^{14}C radiocarbon dates from Baoxiu peat.

Depth (cm)	Material dated	Conventional age (yr BP)	Calibration age (cal yr BP)
76	Grass root	15,360 ± 110	18,439 ± 311
96	Grass root	19,160 ± 120	22,954 ± 295
120	Grass root	23,040 ± 360	27,595 ± 527
162	Grass root	23,770 ± 350	28,709 ± 485
196	Grass root	27,610 ± 490	32,303 ± 441

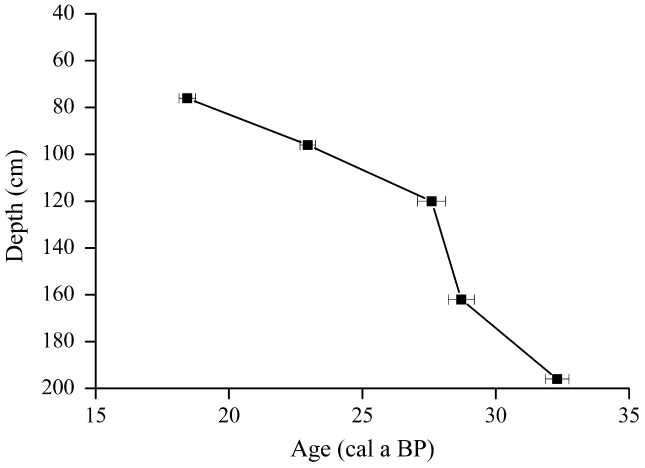

Fig. 3. Age model for the Baoxiu peat sedimentary sequence.

The ash samples were digested with an HNO_3 + HF acid mixture, and the solutions were analyzed for major and trace element concentrations. Major element concentrations were measured on a Varian Vista Pro inductively coupled plasma–atomic emission spectrometer (ICP–AES) at the State Key Laboratory of Geochemistry in the Guangzhou Institute of Geochemistry, Chinese Academy of Sciences (CAS). Trace element concentrations were measured using a Perkin-Elmer Elan 6000 inductively coupled plasma–mass spectrometer (ICP–MS) at the same laboratory. Major and trace element analyses followed the methods described by Liu et al. (1996) and Li et al. (2002), respectively. The precision for major elements was better than 1% (Li et al., 2002), and for trace elements was generally better than 5% (Liu et al., 1996). Several USGS and Chinese soil and sediment reference standards, including GSS-5, GSS-7, and GXR-6 (soils), and GSD-9 and GSD-12 (sediments), were repeatedly measured along with the samples, yielding values that were generally within ±10% (RSD) of the certified values. For further details on the method and results of major and trace element analyses see Wei et al. (2012).

The mineral composition of the bulk sediment samples was measured using a Rigaku D/max-1200 diffractometer at the Guangzhou Institute of Geochemistry, CAS. X-ray diffraction (XRD) patterns of the samples were recorded between 1.5° and 70° (2 h) at a scanning speed of 2°/min with Cu/Kα radiation (30 mA and 40 kV).

The total organic carbon (TOC) content and the $\delta^{13}C_{TOC}$ values of the samples were determined using a Vario EL III elemental analyzer By Lu (2003).

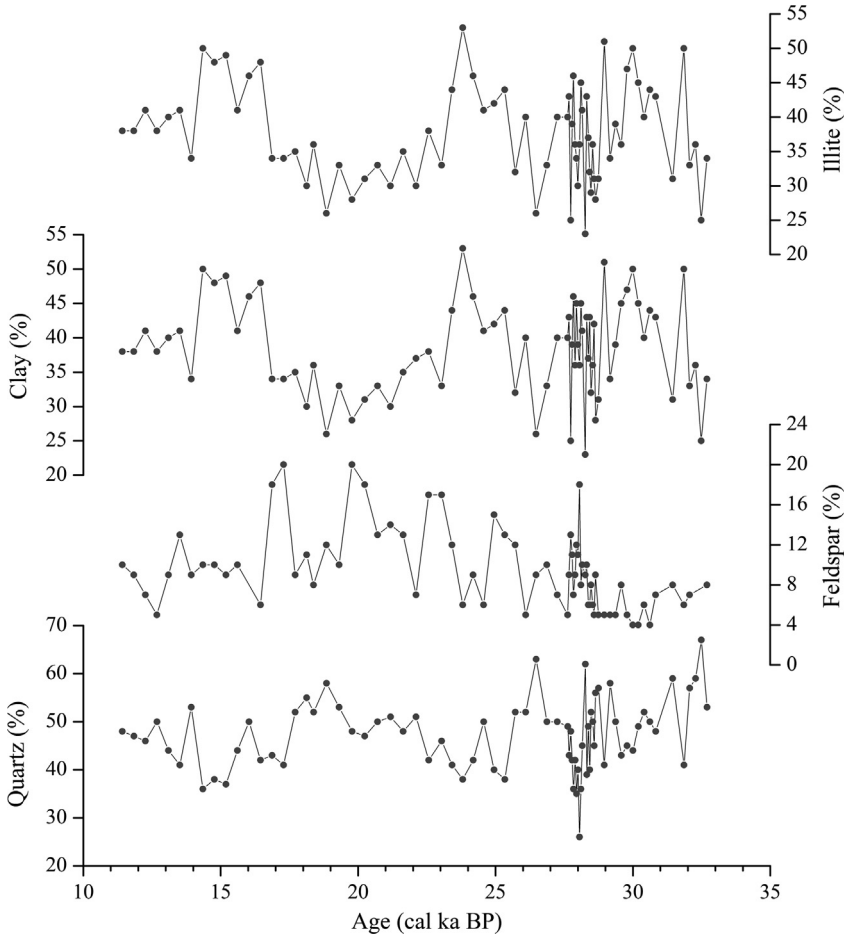

Fig. 4. Relative percentages of quartz, feldspar, clay, and illite versus age in the Baoxiu peat core.

4. Results

Quartz (average concentration = 47.2%), feldspar (9.4%), and clay minerals (38.4%) constitute most of the detrital material found at Baoxiu peat (Fig. 4). Illite is the dominant clay mineral and is present in all sediment samples at concentrations of 23–53%. Smectite and kaolinite are present in only some of the samples, in almost negligible concentrations. The concentrations of quartz, feldspar, and clay range from 26% to 67%, from 4% to 20%, and from 19.4% to 44.3%, respectively. Clay/feldspar ratios range from 0.2 to 1.2 (Fig. 5f). K/Rb, K_2O/Na_2O, and La/Sm ratios are illustrated in Fig. 5c–e, respectively. They show similar patterns of variation throughout the core. The K/Rb ratio varies between 85.3 and 141.5 with a mean value of 103.9. K_2O/Na_2O ratios range from 6.6 to 24 with a mean value of 15.3, and La/Sm ratios range from 4.7 to 5.7 with a mean value of 5.1.

In the Baoxiu core, $\delta^{13}C_{TOC}$ values vary between −26.3‰ and −24.3‰ with a mean of −25.4‰ (Fig. 5b). TOC concentrations vary between 6.6‰ and 44.5‰ with a mean of 23.8‰ (Fig. 5a). Notably, these palaeorecords are punctuated by marked decreases in K/Rb, K_2O/Na_2O, La/Sm, and clay/feldspar ratios, low $\delta^{13}C_{TOC}$ values, and high TOC concentrations.

5. Discussion

5.1. Environmental significance of the proxies

5.1.1. Minerals, and major and trace elements

Clay minerals are secondary minerals that form by the alteration of feldspar, pyroxene, hornblende, and mica (Chamley, 1989). Thus, an increasing weight percent of clay minerals relative to feldspar should be indicative of intensified chemical weathering, possibly induced by enhanced rainfall (Wan et al., 2006). Thus, we use the clay/feldspar ratio as a proxy for the intensity of chemical weathering.

Some major and trace elements (e.g., K, Na, Rb, Zn, Pb, Ti, La, and Sm) behave differently to each other during chemical weathering processes and thus can be used to infer the intensity of chemical weathering. Elemental ratios are more useful than single elements, given the elimination of dilution effects by other components (Nath et al., 2000; Wei et al., 2004). K_2O/Na_2O, K/Rb, and La/Sm ratios are regarded as good proxy indicators for chemical weathering intensity (Nesbitt et al., 1980; Nesbitt and Markovics, 1997; Wei et al., 2004). Most importantly, the use of K_2O/Na_2O and K/Rb ratios in constructing records of chemical

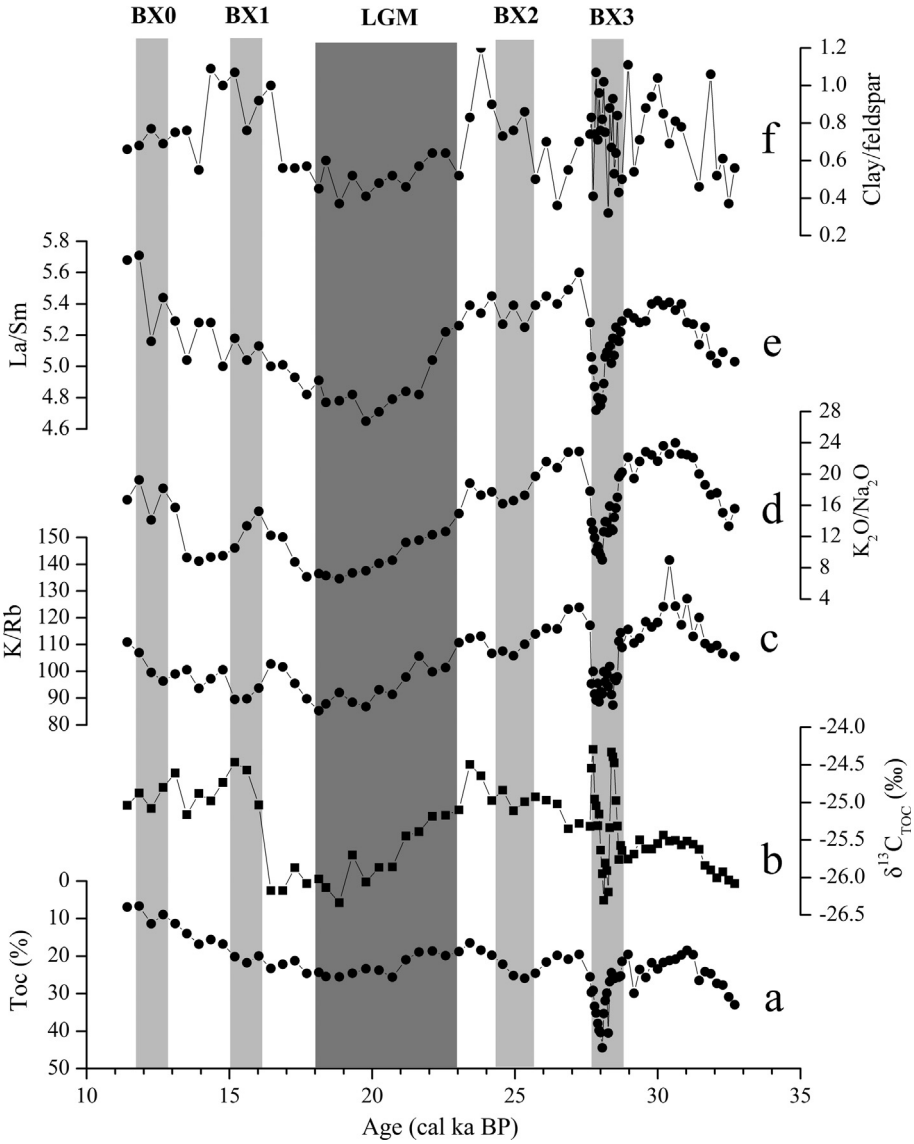

Fig. 5. Multi-proxy record from Baoxiu peat plotted against ages. Events BX0 to BX3 represent intervals of inferred abrupt climate change. LGM = the Last Glacial Maximum.

weathering intensity in the Baoxiu peat has been corroborated by Wei et al. (2012).

5.1.2. Organic proxy record

TOC concentration is a fundamental proxy for the delivery and accumulation of organic matter in sediments (Meyers, 2003). In lake and bog systems, TOC concentrations primarily reflect the degree of organic matter preservation relative to its degradation (Meyers and Ishiwatari, 1993; Wang and Ji, 1995; Meyers and Lallier-Vergès, 1999), which is influenced by climatic factors, namely precipitation and temperature. Consequently, TOC concentrations can serve as a proxy of climatic variations in a region. Peat formation is controlled not only by the deposition of plant residue, but by the decomposition of organic matter via microbiological activity (Chai, 1990). Under warm and wet climatic conditions, the enhancement of microbial reworking and hydrolysis of organic matter would result in lower TOC concentrations. In contrast, dry and cool climatic conditions would inhibit the degradation of peat sediment, water column bacterial activity, and post-depositional microbial reworking of organic matter, and would eventually result in the improved preservation of organic matter in peat deposits (Zhou et al., 2005). Consequently, higher TOC concentrations should indicate drier and cooler conditions, whereas lower TOC contents should indicate wetter and warmer environments, as supported by data from the Dingnan, Dahu, and Dajiuhu peat deposits (Zhou et al., 2004, 2005).

The $\delta^{13}C_{TOC}$ values in the Baoxiu peat core range from −26.3‰ to −24.3‰ (Fig. 5b), consistent with the typical carbon isotope signatures of C3 series plants. The climatic significance of stable carbon isotope compositions in peat bogs is debated (Hong et al., 2005, 2014a, 2014b; Zhu et al., 2009b; Huang, 2015). Huang et al. (2013) proposed that the climatic significance of $\delta^{13}C$ values in peat bogs may vary from region to region, and that independent studies of modern processes are required to properly ascertain the relationship between $\delta^{13}C_{TOC}$ values and climate factors in a certain location. Various factors can influence the $\delta^{13}C$ value of plant tissue, but in certain ecosystems and locations many of these factors are nearly constant or their differences are negligible (Skrzypek et al., 2007a, 2010), and precipitation and temperature are considered the main controlling factors (Menot and Burns, 2001; Skrzypek et al., 2007b, 2011; Loisel et al., 2009; Tillman et al., 2010; Holzkämper et al., 2012). Wang et al. (2013) reported a strong relationship between mean annual temperature and $\delta^{13}C$ values in C3 plants sampled from the 400 mm mean annual precipitation isoline in north China. Indeed, many studies have reported that temperature is the main factor affecting the carbon isotopic composition of peat plants (Skrzypek et al., 2007b, 2011; Tillman et al., 2010; Holzkämper et al., 2012; Huang, 2015). Accordingly, $\delta^{13}C$ time series data from the Altay peat core, north Xinjiang, are thought to provide a continuous proxy record of surface air temperature since 11.5 ka BP (Huang, 2015). A $\delta^{13}C$ record from a peat core from Hala Izerska BP (SW Poland) is also interpreted as having a dominant temperature control (Skrzypek et al., 2009). $\delta^{13}C$ values from peat cores from subarctic Canada, northeast European Russia, and Dürres Maar (Germany) are thought to be controlled mainly by the temperature during the local growing season (Tillman et al., 2010, 2013; Moschen et al., 2011). Thus, it is likely that temperature is the most significant signal in the $\delta^{13}C_{TOC}$ records from the Baoxiu peat core.

5.2. Climate evolution, as recorded in Baoxiu peat

The degree of chemical weathering in a given area is strongly affected by climate. Warm and humid climate conditions promote intensive chemical weathering, with humidity playing a particularly important role (Berner and Berner, 1997). Since Yunnan is influenced by the ISM, the record of chemical weathering intensity in the Baoxiu peat could reflect variations in the ISM. In terms of overall trends, TOC concentrations, $\delta^{13}C_{TOC}$ values, and K/Rb, K_2O/Na_2O, La/Sm, and clay/feldspar ratios show similar variations throughout the entire peat core (Fig. 5). Variations in the ISM inferred from these weathering indices can be roughly divided into three stages, as follows.

(1) *33–23 ka BP*

The period 33–23 ka BP corresponds to the end of Marine Isotope Stage 3 (MIS3) and the onset of MIS2. Ratios of K/Rb, K_2O/Na_2O, La/Sm, and clay/feldspar are relatively high, indicating a higher variability in chemical weathering, likely a result of an intense ISM. The TOC concentrations range from 16.5% to 44.5% and are variable. $\delta^{13}C_{TOC}$ values vary by almost 2.5‰ with an overall rise from about −26.5‰ to −24‰, suggesting warm climatic conditions. Superimposed on the generally high values of weathering indices for the Baoxiu peat are two short-term fluctuations (BX2 and BX3) that indicate minor variability in chemical weathering.

(2) *23–18 ka BP*

The interval 23–18 ka BP corresponds to the LGM, and two dating control points (18,439 ± 311 and 22,954 ± 295 Cal yr BP corresponding to the depth of 76 and 96 cm, respectively) in Baoxiu peat core just can well constrain the timing of the LGM. $\delta^{13}C_{TOC}$ values are more negative, probably as a result of lower temperatures. K/Rb, K_2O/Na_2O, La/Sm, and clay/feldspar ratios are significantly lower during this period than during the previous period, possibly influenced by a weak ISM, resulting in less intense chemical weathering. Dry and cool climatic conditions would suppress the degradation of peat sediments, water column bacterial activity, and post-depositional microbial reworking of organic matter, and may have eventually resulted in high TOC concentrations.

(3) *18–11.4 ka BP*

The interval 18–11.4 ka BP corresponds to the last deglacial. K/Rb, K_2O/Na_2O, La/Sm, and clay/feldspar ratios show a rapid return to a gradually increasing trend, pointing to humid conditions. Interestingly, $\delta^{13}C_{TOC}$ values show a positive excursion, suggesting warmer conditions. TOC concentrations show a gradual decrease, most likely as a result of the warm and wet climatic conditions, which favor the degradation of organic matter. Superimposed on the curves for most of the weathering indices are two fluctuations (BX1 and BX2) that indicate minor variability in chemical weathering conditions.

5.3. Phase relationship between ISM and EASM

The phase relationship between the ISM and EASM on different timescales is complex. Recent studies have attempted to decipher the phase relationship between the two monsoonal systems; however, evidence for both an in-phase (Zhao et al., 2009; Zhang et al., 2011) and an anti-phase (Hong et al., 2005; Wang et al., 2010) relationship during the Holocene has been proposed. Furthermore, few studies have considered the phase relationship between the two during the last glacial. The ISM conditions inferred from pollen records from Xingyun Lake show an out-of-phase relationship with the EASM during the last glaciation (Chen et al., 2014). Stalagmite $\delta^{18}O$ time series from Sanxing also record a decoupling between the ISM and EASM over the interval 20–17 ka BP (Jiang et al., 2014). Interestingly, however, coherent variations in the ISM and EASM on millennial and longer timescales are captured in stalagmite $\delta^{18}O$ records (Jiang et al., 2014).

5.3.1. Synchronous long-term changes in ISM and EASM, and abrupt climatic events

Variations in the Asian monsoon respond predominantly to changes in Northern Hemisphere summer insolation on orbital timescales, as indicated from stalagmite $\delta^{18}O$ time series data (Wang et al., 2001, 2008; Yuan et al., 2004; Cheng et al., 2009). Lacustrine sediment records from Lugu also indicate that long-term paleoenvironment changes respond strongly to solar insolation (Wang et al., 2014). Increased summer insolation in the subtropics tends to enhance land–sea pressure gradients and thus the strength of the ISM. Our geochemical proxy records also broadly suggest orbital-induced variations in summer insolation. Because an enhanced ISM favors intensive chemical weathering, weathering-sensitive geochemical proxies, such as K/Rb ratios in continental sediments, will record such variations.

Variations in the K/Rb ratios in the peat core from this study are shown in Fig. 6, together with total reflectance (L^*) records from the Arabian Sea, which indicate the strength of the ISM (Deplazes et al., 2013, 2014), stalagmite $\delta^{18}O$ time series data from Hulu cave (Wang et al., 2001), and time series records of summer precipitation as reconstructed from carbon isotope ratios in organic matter from the Yuanbao Loess profile (Rao et al., 2013), which are believed to reflect changes in the strength of the EASM. All exhibit synchronous variations on orbital timescales. This suggests that long-term climate variability was broadly synchronous between the ISM and EASM regions, and controlled mainly by changes in Northern Hemisphere summer insolation on orbital scales.

Superimposed on the first-order insolation-driven relationship, our record of K/Rb ratios is punctuated by several distinct millennial-scale events during the last glacial period. These appear to be similar to the weak summer monsoon signals seen in the Hulu cave speleothems (Wang et al., 2001), the Yuanbao Loess profile (Rao et al., 2013), records of total reflectance (L^*) from the Arabian sea (Deplazes et al., 2013, 2014), the Sanxing stalagmite $\delta^{18}O$ record (Jiang et al., 2014), and various cold event signals in Greenland ice cores (Andersen et al., 2004; Svensson et al., 2008) (Fig. 6). Records of the proportion of the >30 μm grain-size fraction from Xingyun Lake, Southwest China, also record the H1, H2, and H3 events (Wu et al., 2015). Four cold events, referred to here as BX0, BX1, BX2, and BX3, can be identified from the K/Rb ratio time series of the Baoxiu peat, and these roughly correspond to the YD, H1, H2, and H3 events, respectively (Bond et al., 1997). Although

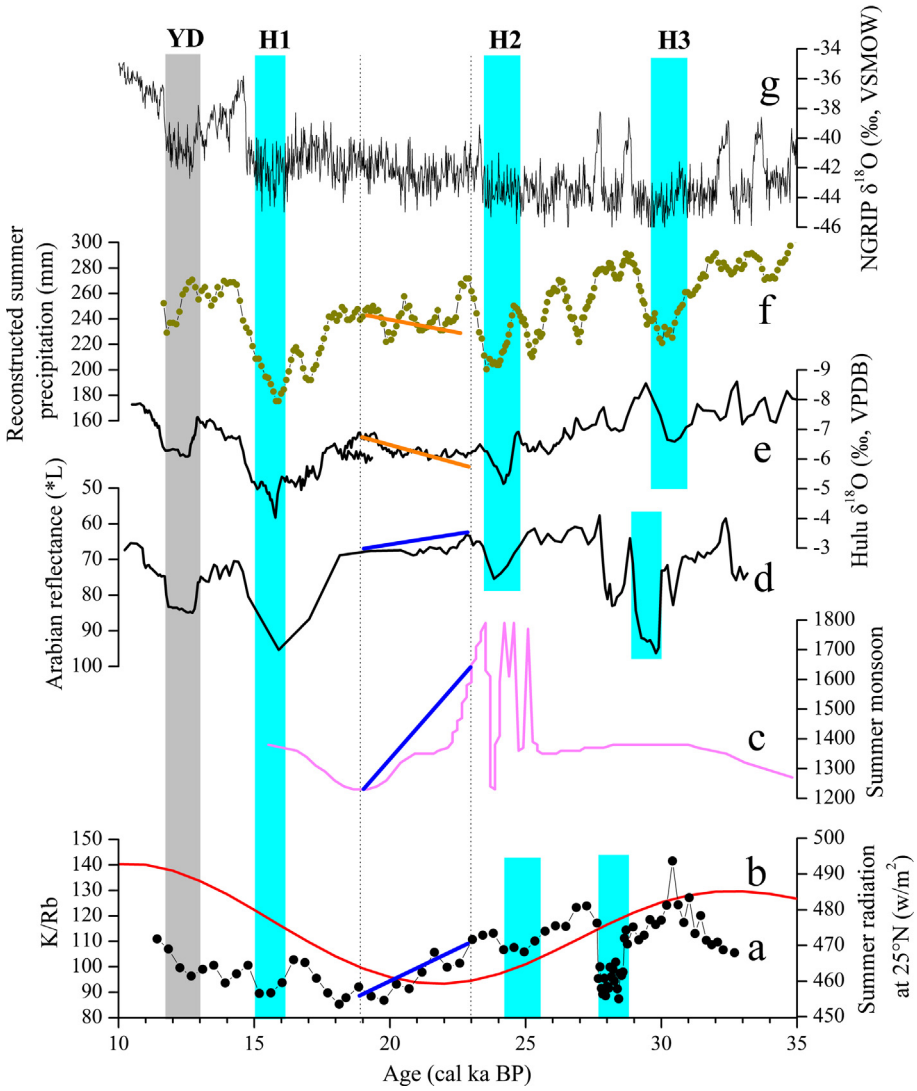

Fig. 6. Comparison of related records: (a) K/Rb ratio from the Baoxiu peat; (b) summer insolation at 25°N latitude (Laskar et al., 2004); (c) summer monsoon reconstructed from the Darjeeling foothill region (Ghosh et al., 2015); (d) record of sediment color from the Arabian Sea (500-point running average; Deplazes et al., 2013); (e) Hulu stalagmite $\delta^{18}O$ record (Wang et al., 2001); (f) reconstructed summer precipitation at Yuanbao Loess profile (Rao et al., 2013); and (g) NGRIP ice-core $\delta^{18}O$ record with GICC05 chronology (Andersen et al., 2004; Svensson et al., 2008). Vertical cyan bars denote the YD and Heinrich events. (For interpretation of the references to color in this figure legend, the reader is referred to the web version of this article.)

there are time offsets between the abrupt, weak ISM signals in the Baoxiu peat records and the cold events detected in the North Greenland Ice Core, these could have resulted from differences in the age models between the two records and possibly different responses of the proxies to climatic/environmental changes. The broad occurrence of these events in different monsoonal regions suggests that the ISM and EASM were in phase during these rapid climatic events.

Periods of increased precipitation, as recorded in speleothem calcite from southern Brazil, are synchronous with the intervals of weakened ISM and EASM (Wang et al., 2001, 2006, 2007; Deplazes et al., 2014). The anti-phase pattern between rainfall in South America and the Asian monsoon region is best explained by a southward shift of the intertropical convergence zone (ITCZ) (Wang et al., 2006, 2007). The abrupt climate changes seen in our records correspond closely to the wet periods recorded in stalagmite $\delta^{18}O$ data from Brazil (Wang et al., 2006, 2007), which also correspond to Heinrich events in the North Atlantic (Bond et al., 1997). Many studies have found that ISM and EASM precipitation patterns are related to variations in North Atlantic climate (Cosford et al., 2008; Deplazes et al., 2013; Marzin et al., 2013; Tierney and Pausata, 2015). The mechanism could explain the millennial-scale teleconnection between the North Atlantic, Asian monsoon region, and South America. Cooling in the North Atlantic could induce a substantially weakened Atlantic Meridional Overturning Circulation (AMOC) and result in a southward shift of the ITCZ and associated changes in Hadley cells (Chiang et al., 2003; Chiang and Bitz, 2005; Zhang and Delworth, 2005). The southward shift in the location of the ITCZ and the zonal-mean Hadley cell would result in weaker ISM and EASM, and wetter conditions at low latitudes in South American.

5.3.2. Anti-phase relationship between the ISM and EASM during ~23–19 ka BP

Stalagmite $\delta^{18}O$ records from Hulu show a negative excursion during the interval 23–19 ka BP, indicating an unusually strong EASM (Wang et al., 2001). An increase in monsoon rainfall during this period is also recorded in sediments of the Yuanbao Loess on the western edge of the Chinese Loess Plateau (Rao et al., 2013). A ^{10}Be record from a Luochuan Loess profile in central China gives further evidence for a strong summer monsoon from 23 to 19 ka BP (Zhou et al., 2007). However, various proxy climate indicators from both terrestrial and marine sediments suggest a weakening of the ISM during this time. Quantitative paleo-precipitation reconstructions in the eastern Himalayas show a clear decrease from 23 to 19 ka BP, indicating a weakening of the ISM (Ghosh et al., 2015). Similarly, a high-resolution analysis of diatoms from Lugu Lake suggests a weakening of the ISM at this time (Wang et al., 2014). TOC records (Schulz et al., 1998) and total reflectance (L^*) data (Deplazes et al., 2013) from the Arabian Sea provide additional evidence for a weak ISM during 23–19 ka BP. Seawater $\delta^{18}O$ and Ba/Ca records from sediment core SK 168/GC-1 in the Andaman Sea suggest that the climate during 23–19 ka BP was characterized by a extremely weak ISM circulation and strongly reduced runoff (Gebregiorgis et al., 2016) A positive excursion from the same interval in stalagmite $\delta^{18}O$ records from Sanxing also suggests a weakened ISM (Jiang et al., 2014). K/Rb ratios from Baoxiu peat in this study are also significantly lower between 23 and 19 ka BP, indicating very dry climatic conditions resulting from a weak ISM.

El Niña-like patterns in the tropical Pacific Ocean could provide a mechanism for the inverse phase relationship between the ISM and EASM. Modern meteorological data also support an inverse phase relationship on annual to decadal timescales (Liu et al., 2008). The results of statistical analyses of the relationship between ISM rainfall and ENSO over the past 100 years indicate that ISM rainfall tends to be reduced during El Niña years (Shukla and Paolino, 1983). Indeed, a particular simulation suggested that severe droughts in India have always been accompanied by El Niña events (Kumar et al., 2006). Stott et al. (2002) proposed that ENSO variations in the west Pacific warm pool during the last glacial are analogous to those of the present day. Investigations of SSTs in the cold tongue of the eastern equatorial Pacific have confirmed that the LGM (23–19 ka) was marked by a decreased SST gradient, weakened Hadley and Walker circulations, a southward shift of the ITCZ, and a persistent El Niña-like pattern in the tropical Pacific (Koutavas et al., 2002), concurrent with the strengthened EASM and weakened ISM.

Currently, investigations into the phase relationship between paleo-monsoon and paleo-ENSO conditions over the last glacial are hampered by the scarcity of high-resolution records. Some studies suggest that the inverse phase relationship between the EASM and the ISM on millennial timescales is linked to the occurrence of El Niña-like conditions in the tropical Pacific during the Holocene (Hong et al., 2005, 2009), although evidence remains limited. Additional sensitive proxies, high-resolution records, and detailed modeling simulations are needed to fully understand the mechanism that underpinned the inverse phase relationship between the two monsoon systems during the last glacial.

5.4. A cool, dry climate with weaker monsoons during the LGM

Multi-proxy records, including TOC concentrations, $\delta^{13}C_{TOC}$ values, and K/Rb, K_2O/Na_2O, La/Sm, and clay/feldspar ratios, from Baoxiu peat suggest harsh climatic conditions, namely relating to the Last Glacial Maximum (LGM), from 23 to 18 ka BP. The K/Rb, K_2O/Na_2O, La/Sm, and clay/feldspar ratios in Baoxiu peat are relatively low during the LGM, indicating less intense chemical weathering and thus a dry climate. $\delta^{13}C_{TOC}$ values show a strongly negative excursion, thus suggesting that the climate was also cold around this time. Similar climatic patterns have been interpreted from a variety of paleoclimate records in southwest China. Climate records inferred from diatom and pollen data from Lugu Lake indicate a dry and cold climate over the LGM (Wang et al., 2014). Reductions in temperature and precipitation during this interval are also inferred from a fluvial sedimentary sequence from the eastern Himalayas (Ghosh et al., 2015), and multi-proxy records from cores from Lake Chen Co indicate that cold, dry conditions prevailed over the LGM (Zhu et al., 2009a). Significantly, based on a review of 75 time series datasets from monsoonal central Asia, Herzschuh (2006) argued that the LGM was characterized by dry or moderately dry climate conditions. Furthermore, modeling provides strong evidence for dry and cold climate conditions during the LGM period in the Asian monsoon region (Jiang and Lang, 2010; Jiang et al., 2011; Chabangborn et al., 2014).

Conversely, some workers have proposed that cold and humid conditions occurred during the LGM. Such conditions have been inferred from, for example, pollen records from Xihu Lake and Dianchi Lake (Lin et al., 1986; Wu et al., 1991) and multi-proxy sediment records from Heqing Lake and Napahai Lake (Jiang et al., 1998; Yin et al., 2002). It is worth noting, however, that these records are relative low in resolution and have large age uncertainties. Indeed, Xiao et al. (2014b) suggested that the causes of these varying descriptions of climatic conditions during the LGM in the regions affected by the ISM are related to sampling at a low temporal resolution, large age uncertainties, regional sensitivity, and even different interpretations of proxy data.

In light of the above, we conclude that southwest China probably experienced a dry and cold climate over the LGM period. More robust records with high temporal resolution and precise chronology are needed to better understand the climatic character of the LGM.

6. Conclusion

The Baoxiu peat record presented in this study provides a complete paleoclimatic record for the interval spanning 32.7–11.4 ka BP, and extends our understanding of regional climatic and environmental change in southwest China. Based on multi-proxy analysis that includes TOC concentrations, $\delta^{13}C_{TOC}$ values, and K/Rb, K_2O/Na_2O, La/Sm, and clay/feldspar ratios, the climate evolution in southwest China can be roughly divided into three stages. During the interval 32.7–23 ka BP, the climate was relative warm and humid. From 23 to 18 ka BP, conditions appear to have been extremely cold and dry. During the interval 18–11.4 ka BP, increasingly warm and humid conditions developed. These peat deposits show an in-phase relationship between the ISM and EASM during the last glacial period on both orbital scales and over abrupt millennial-scale events. However, an inverse phase relationship between the two has been detected in various records during 23–19 ka BP, probably associated with the development of El Niño-like conditions. Significantly, the timing and nature of climatic changes at the LGM remain poorly constrained due to the low temporal resolution of existing records and large uncertainties in their chronology. Therefore, to fully understand the phase relationship between the two monsoon systems and associated mechanisms, along with the climatic characteristics and timing of the LGM in southwest China, more robust, high-resolution records with precise chronologies are needed for the interval spanning the LGM.

Acknowledgement

The authors thank Dr. Tu Xianglin of the State Key Laboratory of Isotope Geochemistry, GIG-CAS, for his assistance with the ICP-MS measurements and to Aaron Stallard for improving the English of the manuscript. This work was financially supported by the National Natural Sciences Foundation of China (41325012 and 41421062), the National Basic Research Program of China (2013CB956103), and the GIG-CAS 135 project 135PY201605. This work is contribution No. IS-2298 from GIG-CAS.

References

An, Z.S., Clemens, S.C., Shen, J., Qiang, X.K., Jin, Z.D., Sun, Y.B., Prell, W.L., Luo, J.J., Wang, S.M., Xu, H., Cai, Y.J., Zhou, W.J., Liu, X.D., Liu, W.G., Shi, Z.G., Yan, L.B., Xiao, X.Y., Chang, H., Wu, F., Ai, L., Lu, F.Y., 2011. Glacial-interglacial India Ann summer monsoon dynamics. Science 333 (6043), 719–723.

Andersen, K.K., Azuma, N., Barnola, J.M., Bigler, M., Biscaye, P., Caillon, N., et al., 2004. High-resolution record of Northern Hemisphere climate extending into the last interglacial period. Nature 431 (7005), 147–151.

Berner, R.A., Berner, E.K., 1997. Silicate weathering and climate. In: Ruddiman, W.F. (Ed.), Tectonic Uplift and Climate Change. Plenum Press, New York, pp. 353–365.

Bond, G., Showers, W., Cheseby, M., Lotti, R., Almasi, P., Demenocal, P., Priore, P., Cullen, H., Hajdas, I., Bonani, G., 1997. A pervasive millenniale scale cycle in north Atlantic Holocene and glacial climates. Science 278, 1257–1266.

Chabangborn, A., Brandefelt, J., Wohlfarth, B., 2014. Asian monsoon climate during the Last Glacial Maximum: palaeo-data-model comparisons. Boreas 43 (1), 220–242.

Chai, X., 1990. Peat-Geology. Geological Publishing House, Beijing, pp. 136–309 (in Chinese).

Chamley, H., 1989. Clay Sedimentology. Springer-Verlag, Berlin.

Chen, X.M., Chen, F.H., Zhou, A.F., Huang, X.Z., Tang, L.Y., Wu, D., Zhang, X.J., Yu, J.Q., 2014. Vegetation history, climatic changes and Indian summer monsoon evolution during the Last Glaciation (36,400–13,400 cal yr BP) documented by sediments from Xingyun Lake, Yunnan, China. Palaeogeogr. Palaeoclimatol. Palaeoecol. 410, 179–189.

Cheng, H., Edwards, R.L., Broecker, W.S., Denton, G.H., Kong, X.G., Wang, Y.J., Zhang, R., Wang, X.F., 2009. Ice age terminations. Science 326 (5950), 248–252.

Chiang, J.C., Biasutti, M., Battisti, D.S., 2003. Sensitivity of the Atlantic Intertropical Convergence Zone to Last Glacial Maximum boundary conditions. Paleoceanography 18 (4).

Chiang, J.C., Bitz, C.M., 2005. Influence of high latitude ice cover on the marine Intertropical Convergence Zone. Clim. Dyn. 25 (5), 477–496.

Cook, C.G., Jones, R.T., Langdon, P.G., Leng, M.J., Zhang, E.L., 2011. New insights on Late Quaternary Asian palaeomonsoon variability and the timing of the Last Glacial Maximum in southwestern China. Quatern. Sci. Rev. 30 (7–8), 808–820.

Cook, C.G., Leng, M.J., Jones, R.T., Langdon, P.G., Zhang, E., 2012. Lake ecosystem dynamics and links to climate change inferred from a stable isotope and organic palaeorecord from a mountain lake in southwestern China (ca. 22.6–10.5 cal ka BP). Quatern. Res. 77 (1), 132–137.

Cosford, J., Qing, H.R., Yuan, D.X., Zhang, M.L., Holmden, C., Patterson, W., Cheng, H., 2008. Millennial-scale variability in the Asian monsoon: Evidence from oxygen isotope records from stalagmites in southeastern China. Palaeogeogr. Palaeoclimatol. Palaeoecol. 266 (1–2), 3–12.

Danzeglocke, U., Jöris, O., Weninger, B., 2010. CalPal-2007^{online}. <http://www.calpalonline.de/> (accessed 15.10.10).

Deplazes, G., Lückge, A., Peterson, L.C., Timmermann, A., Hamann, Y., Hughen, K.A., Röhl, U., Laj, C., Cane, M.A., Sigman, D.M., Haug, G.H., 2013. Links between tropical rainfall and North Atlantic climate during the last glacial period. Nat. Geosci. 6 (3), 213–217.

Deplazes, G., Lückge, A., Stuut, J.B.W., Pätzold, J., Kuhlmann, H., Husson, D., Fant, M., Haug, G.H., 2014. Weakening and strengthening of the Indian monsoon during Heinrich events and Dansgaard-Oeschger oscillations. Paleoceanography 29 (2), 99–114.

Ding, Y., Chan, J.C.L., 2005. The East Asian summer monsoon: an overview. Meteorol. Atmos. Phys. 89 (1–4), 117–142.

Gao, Y.X., Xu, S.Y., Guo, Q.Y., 1962. In: Gao, Y.X., Xu, S.Y. (Eds.), Some Problems of East Asian Monsoon. Science Press, Beijing, pp. 49–63 (in Chinese).

Gebregiorgis, D., Hathorne, E.C., Sijinkumar, A.V., Nath, B.N., Nürnberg, D., Frank, M., 2016. South Asian summer monsoon variability during the last ~54 kyrs inferred from surface water salinity and river run off proxies. Quatern. Sci. Rev. 138, 6–15.

Ghosh, R., Bera, S., Sarkar, A., Paruya, D.K., Yao, Y.F., Li, C.S., 2015. A ~50 ka record of monsoonal variability in the Darjeeling foothill region, eastern Himalayas. Quatern. Sci. Rev. 114, 100–115.

Herzschuh, U., 2006. Palaeo-moisture evolution in monsoonal Central Asia during the last 50,000 years. Quatern. Sci. Rev. 25 (1–2), 163–178.

Holzkämper, S., Tillman, P.K., Kuhry, P., Kuhry, P., Esper, J., 2012. Comparison of stable carbon and oxygen isotopes in Picea glauca tree rings and Sphagnum fuscum moss remains from subarctic Canada. Quatern. Res. 78 (2), 295–302.

Hong, B., Gasse, F., Uchida, M., Hong, Y.T., Leng, X.L., Shibata, Y., An, N., Zhu, Y.X., Wang, Y., 2014a. Increasing summer rainfall in arid eastern-Central Asia over the past 8500 years. Sci. Rep. 4, 5279.

Hong, B., Hong, Y.T., Uchida, M., Shibata, Y., Cai, C., Peng, H.J., Zhu, Y.X., Wang, Y., Yuan, L.G., 2014b. Abrupt variations of Indian and East Asian summer monsoons during the last deglacial stadial and interstadial. Quatern. Sci. Rev. 97, 58–70.

Hong, Y.T., Hong, B., Lin, Q.H., Shibata, Y., Hirota, M., Zhu, Y.X., Leng, X.T., Wang, Y., Wang, H., Yi, L., 2005. Inverse phase oscillations between the East Asian and Indian Ocean summer monsoons during the last 12000 years and paleo-El Niño. Earth Planet. Sci. Lett. 231 (3–4), 337–346.

Hong, Y.T., Hong, B., Lin, Q.H., Shibata, Y., Zhu, Y.X., Leng, X.T., Wang, Y., 2009. Synchronous climate anomalies in the western North Pacific and North Atlantic regions during the last 14,000 years. Quatern. Sci. Rev. 28 (9–10), 840–849.

Huang, C., Li, Y.H., Li, Y.X., Guo, W.K., Rao, Z.G., 2013. A review of paleoclimatic changes in China based on peat cellulose isotopic records. Mar. Geol. Quatern. Geol. 33, 113–124 (in Chinese with English abstract).

Huang, C., 2015. Peat cellulose carbon isotopic record and possible driving mechanisms during the past 11.5 ka in Altay, Northern Xinjiang. Thesis for Master's Degree of Lanzhou University.

Jiang, D.B., Lang, X.M., 2010. Last glacial maximum East Asian monsoon: results of PMIP simulations. J. Clim. 23 (18), 5030–5038.

Jiang, D.B., Lang, X.M., Tian, Z.P., Guo, D.L., 2011. Last glacial maximum climate over China from PMIP simulations. Palaeogeogr. Palaeoclimatol. Palaeoecol. 309 (3–4), 347–357.

Jiang, X.Y., He, Y.Q., Shen, C.C., Lee, S.Y., Yang, B., Lin, K., Li, Z.Z., 2014. Decoupling of the East Asian summer monsoon and Indian summer monsoon between 20 and 17 ka. Quatern. Res. 82 (1), 146–153.

Jiang, X.Z., Wang, S.M., Yang, X.D., 1998. Paleoclimatic and environmental changes over the last 30000 years in Heqing Basin, Yunnan Province. J. Lake Sci. 10 (2), 10–16 (in Chinese with English abstract).

Koutavas, A., Lynch-Stieglitz, J., Marchitto, T.M., Sachs, J.P., 2002. El Niño-like pattern in ice age tropical Pacific sea surface temperature. Science 297 (5579), 226–230.

Kramer, A., Herzschuh, U., Mischke, S., Zhang, C., 2010. Late glacial vegetation and climate oscillations on the southeastern Tibetan Plateau inferred from the Lake Naleng pollen profile. Quatern. Res. 73 (2), 324–335.

Kumar, K.K., Rajagopalan, B., Hoerling, M., Bates, G., Cane, M., 2006. Unraveling the mystery of Indian monsoon failure during El Niño. Science 314 (5796), 115–119.

Laskar, J., Robutel, P., Joutel, F., Gastineau, M., Correia, A.C.M., Levrard, B., 2004. A long term numerical solution for the insolation quantities of the Earth. Astron. Astrophys. Manuscr. 428, 261–285.

Li, X.H., Liu, Y., Tu, X.L., Hu, G.Q., Zeng, W., 2002. Precise determination of chemical compositions in silicate rocks using ICP-AES and ICP-MS. A comparative study of sample digestion techniques of alkali fusion and acid dissolution. Geochimica 31 (3), 289–294 (in Chinese with English abstract).

Lin, S.M., Qiao, Y.L., Walker, D., 1986. Late Pleistocene and Holocene vegetation history at Xi Hu, Er Yuan, Yunnan Province, Southwest China. J. Geogr. Sci. 13 (5), 419–440.

Liu, J., Wang, B., Yang, J., 2008. Forced and internal modes of variability of the East Asian summer monsoon. Clim. Past Discuss. 4 (3), 645–666.
Liu, Y., Liu, H.C., Li, X.H., 1996. Simultaneous and precise determination of 40 trace elements in rock samples using ICP-MS. Geochimica 25 (6), 552–558 (in Chinese with English abstract).
Long, R.H., Li, B.F., Brenner, M., Song, X.L., 1991. A study of late Pleistocene to Holocene vegetation in Qilu Lake area of central Yunnan. Geol. Yunnan 10 (1), 105–118 (In Chinese with English abstract).
Loisel, J., Garneau, M., Hélie, J.F., 2009. Modern Sphagnum $\delta^{13}C$ signatures follow a surface moisture gradient in two boreal peat bogs, James Bay lowlands, Québec. J. Quat. Sci. 24 (3), 209–214.
Lu, Y.H., 2003. Carbon Isotopes of the Biomarkers in Peats and their Implications for Climate Changes. Thesis for Master's Degree of Zhejiang University.
Marzin, C., Kallel, N., Kageyama, M., Duplessy, J.C., Braconnot, P., 2013. Glacial fluctuations of the Indian monsoon and their relationship with North Atlantic climate: new data and modelling experiments. Clim. Past 9 (5), 2135–2151.
Menot, G., Burns, S.J., 2001. Carbon isotopes on omborgenic peat bog plants as climatic indicators calibration from an altitudinal transect in Switzerland. Org. Geochem. 32, 233–245.
Meyers, P.A., Ishiwatari, R., 1993. Lacustrine organic geochemistry: an overview of indicators of organic matter sources and diagenesis in lake sediments. Org. Geochem. 20, 867–900.
Meyers, P.A., Lallier-Vergès, E., 1999. Lacustrine sedimentary organic matter records of Late Quaternary paleoclimates. J. Paleolimnol. 21 (3), 345–372.
Meyers, P.A., 2003. Applications of organic geochemistry to paleolimnological reconstructions: a summary of examples from the Laurentian Great Lakes. Org. Geochem. 342, 261–289.
Moschen, R., Kühl, N., Peters, S., Vos, H., Lücke, A., 2011. Temperature variability at Dürres Maar, Germany during the migration period and at high medieval times, inferred from stable carbon isotopes of Sphagnum cellulose. Clim. Past Discuss. 7 (1), 535–573.
Nath, B.N., Kunzendorf, H., Plüger, W.L., 2000. Influence of provenance, weathering, and sedimentary processes on the elemental ratios of the fine-grained fraction of the bedload sediments from the Vembanad Lake and the adjoining continental shelf, Southwest coast of India. J. Sediment. Res. 70 (5), 1081–1094.
Nesbitt, H.W., Markovics, G., Price, R.C., 1980. Chemical processes affecting alka BPlis and alka BPline earths during continental weathering. Geochim. Cosmochim. Acta 44, 1659–1666.
Nesbitt, H.W., Markovics, G., 1997. Weathering of granodioritic crust, long-term storage of elements in weathering profiles, and petrogenesis of siliciclastic sediments. Geochim. Cosmochim. Acta 61 (8), 1653–1670.
Rao, Z.G., Chen, F.H., Cheng, H., Liu, W.G., Wang, G.A., Lai, Z.P., Bloemendal, J., 2013. High-resolution summer precipitation variations in the western Chinese Loess Plateau during the last glacial. Sci. Rep. 3, 2785.
Schulz, H., von Rad, U., Erlenkeuser, H., 1998. Correlation between Arabian Sea and Greenland climate oscillations of the past 110,000 years. Nature 393 (6680), 54–57.
Shen, J., Jones, R.T., Yang, X., Dearing, J.A., Wang, S., 2006. The Holocene vegetation history of Lake Erhai, Yunnan province southwestern China: the role of climate and human forcings. Holocene 16 (2), 265–276.
Shukla, J., Paolino, D.A., 1983. The Southern Oscillation and long-range forecasting of the summer monsoon rainfall over India. Mon. Weather Rev. 111 (9), 1830–1837.
Skrzypek, G., Kałużny, A., Jędrysek, M.O., 2007a. Carbon stable isotope analyses of mosses- comparisons of bulk organic matter and extracted nitrocellulose. J. Am. Soc. Mass Spectrom. 18 (8), 1453–1458.
Skrzypek, G., Kaluzny, A., Wojtun, B., Jędrysek, M.O., 2007b. The carbon stable isotopic composition of mosses: a record of temperature variation. Org. Geochem. 38 (10), 1770–1781.
Skrzypek, G., Baranowska-Kącka, A., Keller-Sikora, A., Jędrysek, M.O., 2009. Sphagnum and temperature negative relationship-Analogous trends in pollen percentages and carbon stable isotope composition of Holocene peat-Possible interpretation for palaeoclimate studies. Rev. Palaeobot. Palynol. 156 (3–4), 507–518.
Skrzypek, G., Jezierski, P., Szynkiewicz, A., 2010. Preservation of primary stable isotopesignatures of peat-forming plants during early decomposition-observation along an altitudinal transect. Chem. Geol. 273, 238–249.
Skrzypek, G., Engel, Z., Chuman, T., Šefrna, L., 2011. Distichia peat-A new stable isotope paleoclimate proxy for the Andes. Earth Planet. Sci. Lett. 307, 298–308.
Stott, L., Poulsen, C., Lund, S., Thunell, R., 2002. Super ENSO and global climate oscillations at millennial time scales. Science 297 (5579), 222–226.
Svensson, A., Andersen, K.K., Bigler, M., Clausen, H.B., Dahl-Jensen, D., Davies, S.M., Johnsen, S.J., Muscheler, R., Parrenin, F., Rasmussen, S.O., Röthlisberger, R., Seierstad, I., Steffensen, J.P., Vinther, B.M., 2008. A 60,000 year Greenland stratigraphic ice core chronology. Clim. Past 4 (1), 47–57.
Tareq, S.M., Kitagawa, H., Ohta, K., 2011. Lignin biomarker and isotopic records of paleovegetation and climate changes from Lake Erhai, southwest China, since 18.5 ka BP. Quatern. Int. 229 (1–2), 47–56.
Tierney, J.E., Pausata, F.S., 2015. Deglacial Indian monsoon failure and North Atlantic stadials linked by Indian Ocean surface cooling. Nat. Geosci. 9 (1), 46–50.
Tillman, P.K., Holzkämper, S., Kuhry, P., Sannel, A.B., Loader, N.J., Robertson, I., 2010. Stable carbon and oxygen isotopes in Sphagnum fuscum peat from subarctic Canada: implications for palaeoclimate studies. Chem. Geol. 270, 216–226.
Tillman, P.K., Holzkämper, S., Andersen, T.J., Hugelius, G., Kuhry, P., Oksanen, P., 2013. Stable isotopes in Sphagnum fuscum peat as late-Holocene climate proxies in northeastern European Russia. Holocene 23 (10), 1381–1390.
Wan, S., Li, A., Clift, P.D., Jiang, H., 2006. Development of the East Asian summer monsoon: Evidence from the sediment record in the South China Sea since 8.5 Ma. Palaeogeogr. Palaeoclimatol. Palaeoecol. 241 (1), 139–159.
Wang, G.A., Li, J.Z., Liu, X.Z., Li, X.Y., 2013. Variations in carbon isotope ratios of plants across a temperature gradient along the 400 mm isoline of mean annual precipitation in north China and their relevance to paleovegetation reconstruction. Quatern. Sci. Rev. 63, 83–90.
Wang, Q., Yang, X., Anderson, N.J., Zhang, E., Li, Y., 2014. Diatom response to climate forcing of a deep, alpine lake (Lugu Hu, Yunnan, SW China) during the Last Glacial Maximum and its implications for understanding regional monsoon variability. Quatern. Sci. Rev. 86, 1–12.
Wang, S.M., Ji, L., 1995. Hulun Lake. Press of Chinese University of Science and Technique, Hefei, pp. 85–93 (in Chinese).
Wang, X.F., Auler, A.S., Edwards, R.L., Cheng, H., Ito, E., Solheid, M., 2006. Interhemispheric anti-phasing of rainfall during the last glacial period. Quatern. Sci. Rev. 25 (23), 3391–3403.
Wang, X.F., Auler, A.S., Edwards, R.L., Cheng, H., Ito, E., Wang, Y.J., Kong, X.G., Solheid, M., 2007. Millennial-scale precipitation changes in southern Brazil over the past 90,000 years. Geophys. Res. Lett. 34 (23), 3391–3403.
Wang, Y.J., Cheng, H., Edwards, R.L., An, Z.S., Wu, J.Y., Shen, C.C., Dorale, J.A., 2001. A high-resolution absolute-dated late Pleistocene monsoon record from Hulu Cave, China. Science 294 (5550), 2345–2348.
Wang, Y.J., Cheng, H., Edwards, R.L., Kong, X.G., Shao, X.H., Chen, S.T., Wu, J.Y., Jiang, X.Y., Wang, X.F., An, Z.S., 2008. Millennial- and orbital-scale changes in the East Asian monsoon over the past 224,000 years. Nature 451 (7182), 1090–1093.
Wang, Y.B., Liu, X.Q., Herzschuh, U., 2010. Asynchronous evolution of the Indian and East Asian Summer Monsoon indicated by Holocene moisture patterns in monsoonal central Asia. Earth Sci. Rev. 103 (3–4), 135–153.
Wei, G.J., Liu, Y., Li, X.H., Shao, L., Fang, D.Y., 2004. Major and trace element variations of the sediments at ODP Site 1144, South China Sea, during the last 230 ka and their paleoclimate implications. Palaeogeogr. Palaeoclimatol. Palaeoecol. 212 (3–4), 331–342.
Wei, G.J., Xie, L.H., Sun, Y.G., Lu, Y.H., Liu, Y., 2012. Major and trace elements of a peat core from Yunnan, Southwest China: implications for paleoclimatic proxies. J. Asian Earth Sci. 58, 64–77.
Wu, D., Zhou, A.F., Chen, X.M., Yu, J.Q., Zhang, J.W., Sun, H.L., 2015. Hydrological and ecosystem response to abrupt changes in the Indian monsoon during the last glacial, as recorded by sediments from Xingyun Lake, Yunnan, China. Palaeogeogr. Palaeoclimatol. Palaeoecol. 421, 15–23.
Wu, Y.S., Chen, Y.S., Xiao, J.Y., 1991. A preliminary study on vegetation and climate changes in Dianchi Lake area in the last 40,000 years. Acta Botan. Sinica 33 (6), 450–458 (In Chinese with English abstract).
Xiao, X.Y., Haberle, S.G., Shen, J., Yang, X.D., Han, Y., Zhang, E.L., Wang, S.M., 2014a. Latest Pleistocene and Holocene vegetation and climate history inferred from an alpine lacustrine record, northwestern Yunnan Province, southwestern China. Quatern. Sci. Rev. 86, 35–48.
Xiao, X.Y., Haberle, S.G., Yang, X.D., Shen, J., Han, Y., Wang, S.M., 2014b. New evidence on deglacial climatic variability from an alpine lacustrine record in northwestern Yunnan Province, southwestern China. Palaeogeogr. Palaeoclimatol. Palaeoecol. 406, 9–21.
Xiao, X.Y., Shen, J.I., Haberle, S.G., Han, Y., Xue, B., Zhang, E.L., Wang, S.M., Tong, G.B., 2015. Vegetation, fire, and climate history during the last 18,500 cal a BP in south-western Yunnan Province, China. J. Quat. Sci. 30 (8), 859–869.
Yin, Y., Fang, N.Q., Sheng, J.F., Hu, C.Y., Nie, H.G., 2002. Lacustrine records of environmental changes during the last 57 ka in the Napahai Lake, Northwestern Yunnan. Mar. Geol. Quatern. Geol. 22 (4), 99–105 (In Chinese with English abstract).
Yuan, D.X., Cheng, H., Edwards, R.L., Dykoski, C.A., Kelly, M.J., Zhang, M.L., Qing, J.M., Lin, Y.S., Wang, Y.J., Wu, J.Y., Dorale, J.A., An, Z.S., Cai, Y.J., 2004. Timing, duration, and transitions of the last interglacial Asian monsoon. Science 304 (5670), 575–578.
Zhang, J.W., Chen, F.H., Holmes, J.A., Li, H., Guo, X.Y., Wang, J.L., Li, S., Lü, Y.B., Zhao, Y., Qiang, M.R., 2011. Holocene monsoon climate documented by oxygen and carbon isotopes from lake sediments and peat bogs in China: a review and synthesis. Quatern. Sci. Rev. 30 (15–16), 1973–1987.
Zhang, R., Delworth, T.L., 2005. Simulated tropical response to a substantial weakening of the Atlantic thermohaline circulation. J. Clim. 18 (12), 1853–1860.
Zhao, Y., Yu, Z.C., Chen, F.H., Zhang, J.W., Yang, B., 2009. Vegetation response to Holocene climate change in monsoon-influenced region of China. Earth Sci. Rev. 97 (1–4), 242–256.
Zhou, W.J., Priller, A., Beck, J.W., Wu, Z.K., Chen, M.B., An, Z.S., Walter, K., Xian, F., Yu, H.G., Liu, L., 2007. Disentangling geomagnetic and precipitation signals in an 80-kyr Chinese loess record of ^{10}Be. Radiocarbon 49 (1), 139.
Zhou, W.J., Xie, S.C., Meyers, P.A., Zheng, Y.H., 2005. Reconstruction of late glacial and Holocene climate evolution in southern China from geolipids and pollen in the Dingnan peat sequence. Org. Geochem. 36 (9), 1272–1284.
Zhou, W.J., Yu, X.F., Jull, A.T., Burr, G., Xiao, J.Y., Lu, X.F., Xian, F., 2004. High-resolution evidence from southern China of an early Holocene optimum and a mid-Holocene dry event during the past 18,000 years. Quatern. Res. 62 (1), 39–48.
Zhu, L.P., Zhen, X.L., Wang, J.B., Lü, H.Y., Xie, M.P., Kitagawa, H., Possnert, G., 2009a. A ~30,000-year record of environmental changes inferred from Lake Chen Co, Southern Tibet. J. Paleolimnol. 42 (3), 343–358.
Zhu, Y., Chen, Y., Zhao, Z.J., Xiao, J.Y., Zhang, M.H., Shu, Q., Zhao, H.Y., 2009b. Record of environmental change by α-cellulose δ13C of sphagnum peat at Shennongjia, 4000–1000 a BP. Chin. Sci. Bull. 54, 3731–3738.